On the Artificial Strip Roughness

AUTHOR(S):

ADACHI, Shohei

CITATION:

ADACHI, Shohei. On the Artificial Strip Roughness. Bulletins - Disaster Prevention Research Institute, Kyoto University 1964, 69: 1-20

ISSUE DATE:

1964-03-25

URL:

http://hdl.handle.net/2433/123743

DISASTER PREVENTION RESEARCH INSTITUTE
BULLETIN No. 69 MARCH, 1964

ON THE ARTIFICIAL STRIP ROUGHNESS

BY

SHOHEI ADACHI

KYOTO UNIVERSITY, KYOTO, JAPAN

DISASTER PREVENTION RESEARCH INSTITUTE
KYOTO UNIVERSITY
BULLETINS

Bulletin No. 69 March, 1964

On the Artificial Strip Roughness

By

Shohei ADACHI

On the Artificial Strip Roughness

By

Shohei ADACHI

Abstract

Using the artificial strip roughness, the roughness effects were investigated. The tests were conducted in the 20 cm wide, 30 cm deep, and 14.4 cm long steel flume with 1/500 slope. The roughness element was a rectangular cross-sectional wooden bar, 5 mm in height and 6.4 mm in width. It was found that the resistance behavior of the strip roughness varied with the relative roughness spacing and that it should be classified into the ridge and the groove roughness. From the measurements of the pressure drag coefficient of the strip roughness element, the practical criterion between the ridge and the groove roughness was proposed. Besed on the conception that the equivalent sand roughnesswas an expression of the wall region where the intense eddies were induced by the roughness elements, the empirical logarithmic roughness formulas were developed.

Introduction

During the past 30 years much research has been carried out on the artificial roughness. While the artificial roughness has been used as the hypothetical model of natural roughness, especially as a controlling tool for the flow resistance in the fixed bed, the choice of patterns of the artificial roughness has been left to the individuals and the lack of information on the choice has caused trouble in the hydraulic experiments involving roughness problems.

So-called equivalent sand roughness based on Nikuradse's uniform sand grain roughness, is a common expression of the roughness effect. Uniform sand grain roughness has a unique simplicity in that both the size and the spacing of the roughness elements can be indicated by the grain diameter. However, the equivalent sand roughness dose not correspond directly to the dimensions of grain size. In regard to this point, many opinions have been

formed. R. W. Powell[1),2)] proposed another roughness scale based on his own experiments using the square cross-sectional roughness elements. M. L. Albertson and others[3)] showed that certain types of roughness, in which the relative spacing, in addition to the relative size of the roughness element, was an important boundary characteristic, had a different nature from the uniform sand grain roughness. H. M. Morris[4),5)] implied that the roughness effects is to be considered as the relative roughness spacing rather than the relative roughness height.

In the author's opinion the value of Nikuradse's k_s, and accordingly the equivalent sand roughness, dose not mean a measure for thd sand grain but a measure for the region close to the wall, namely the wall region, where the intense eddies are induced by the roughness elements. It is, thus, apparent that the equivalent sand roughness does not always correspond to the pattern of the roughness.

The datum plane of the roughness is another important factor in the expression of the roughness effects. In the case of a single roughness element, the datum plane should be set on the flume bottom, On the other hand, if the roughness elements are placed vary close together, the datum plane should be set on the top of the roughness elements.

In this study it was confirmed that the pattern of the flow over the strip roughness varied with the relative roughness spacing. The position of the datum plane was discussed from the sheltering effect of the ridge element and the strip roughness was classified into the ridge and the groove roughness. Finally the empirical logarithmic roughness formulas for these were developed in terms of the relative roughness height and the relative ridge spacing or the relative groove spacing.

Notations

k = height of the strip roughness element.
k_s = grain diameter of Nikuradse's uniform sand roughness, or equivalent sand roughness.
s = spacing of the strip roughness elements.
b = opening length between the ridge elements, or groove width.
c = sheltering height of the ridge element.
t = width of the ridge element.

M=the integral constant in the logarithmic velocity distribution law.

C_D=drag coefficient.

B=width of the flume.

H=flow depth.

R=hydraulic radius.

U=average velocity.

U_*=average shear velocity.

γ=relative flow depth ($=2H/B$).

Other notations are annotated in the text. In addition, in the first test H, R, U, U_* and γ are measured based on the flume bottom and the values of those based on the top of the roughness element are noted after the dash. On the other hand in the second test those are measured based on the top of the roughness element.

Experiments

The general arrangement of the apparatus is shown in Fig. 1. The test flume was a steel channel painted with vinyl paint, 14.4 m long 20 cm wide and 30 cm deep. The flume was clamped to the steel frame at intervals of 2 m and set up at a 1/500 slope. At the end of the flume a tail gate was set in order that the flows could be made uniform through the flume.

The flow profiles were measured by using three point gages at fixed

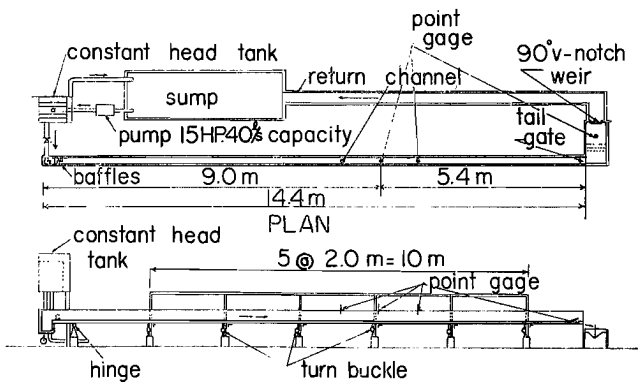

Fig. 1. General view of the experimental apparatus

stations, 9 m, 10 m and 11 m distant from the upstream end of the flume. When the water surface fluctuated remarkably, the piezometer and the auto-stage meter of electric resistance type were used at the same time. The rate of the flow, which ranged from 0.15 l/sec to 15 l/sec, was measured by using a 90° V-notch weir at the outlet of the flume.

The strip roughness elements, having a rectangular cross-section of 5 mm in heigh and 6.4 mm in width, were made from Japanese cypress bars. These elements were placed on the bottom of the flume with constant longitudinal spacing.

The first tests were conducted with the following 6 spacings : 80 cm, 40 cm, 20 cm, 10 cm, 5 cm and 2.5 cm. In order to determine the measurement of the pressure drag force on the roughness element, a fistular brass bar having the same size was provied in addition to the wooden bars. Four small holes of 0.5 mm diameter were drilled in both the upstream and the downstream face at intervals of 1 mm from the bottom. These small holes were independently led to the outside of the flume through the bottom and connected with tilting manometers by vinyl tubes. The pressure drag force was measured from the difference in the pressure head between two faces.

The second tests were conducted with dense roughness elements. At first the bars were placed at intervals of 12.8 mm, twice the bar width. After this pattern, every other opening was filled up with a bar. By the same manner, the groove roughness was formed until the bottom was covered entirely. Then, the groove width was held constant, 6.4 mm, and the widths of the ridge element were 6.4 mm, 19.1 mm, 44.7 mm, 95.7 mm and infinity in that order. Although the top surfaces of the ridge elements were painted at each reformation, some irregularity remained on the surface due to the warp of the bars.

Results and Considerations

(1) Equivalent sand roughness to the strip roughness

The friction factor U/U_* at each relative roughness spacing s/k observed in the first tests, in which s/k ranged from 5 to 160, are plotted against the relative flow depth γ in Fig. 2. The dotted curves in Fig. 2 indicate the relationships between the friction factor and the relative flow

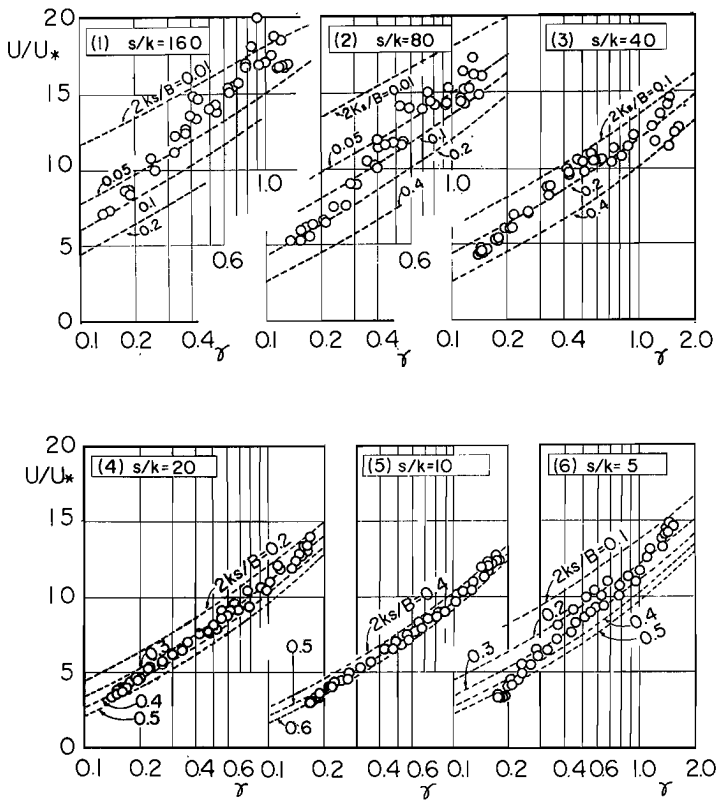

Fig. 2. Relations between U/U_* and γ for various s/k.

depth under the same conditions, but the bottom roughness is constructed by the uniform sand grain, calculated by the author's method[6] with the constants derived from Nikuradse's experiments. If the strip roughness with a constant s/k is equivalent to the resistance to a sand grain roughness, the experimental points should be plotted on a dotted curve. The experimental points of $s/k=10$, Fig. 2 (5), are almost all placed on the curve of $2k_s/B=0.5$. However, with increasing s/k the rows of point, as will be seen, run at an angle to the constant k_s curves. Although the datum plane of the roughness should be reconsidered later, it may be concluded that the strip roughness does not always correspond to Nikuradse's sand roughness ; in other words, the equivalent sand roughness to the strip roughness should be considered as a function of the flow depth.

(2) Patterns of the flow over the strip roughness

The rsistance to flow over a rough surface is generally characterized by the region close to the wall where the intense eddies are induced by the roughness elements. Such a region may be considered as a kind of boundary layer and may be called the wall region. According to the Prandtl and Kármán logarithmic velocity distribution law, mean velocity u at a distance z from the wall is given in the following form.

$$u/u_* = (1/\kappa)\ln(Mz) \tag{1}$$

in which u_* is shear velocity and κ is Kármán constant, 0.4. Referring to Nikuradse's experiment, the constant M is given as

$$M = 30/k_s, \tag{2}$$

in which k_s is the so-called equivalent sand roughness. Since M depends essentially on the behavior of the wall region, equivalent sand roughness is to be considered as a paramenter of the wall region.

H. M. Morris[4),5)] classified the flow patterns on a rough surface into three types. They are skimming flow (or quasi-smooth flow), wake-interference flow (or hyper-turbulent flow), and isolated roughness flow (or semi-smooth turbulent flow). Skimming flow occurs when the roughness elements are so close together that the flow essentially skims over the top of the elements. In such a flow, the wall region will be similar to the laminar sublayer on the smooth surface. Wake-interference flow occurs when the roughness elements are placed so close together that the wakes at each element interfere with those developed at the following element, resulting in the uniform wall region. It would seem that a typical example of this flow pattern might be that with the uniform sand grain roughness. Isolated-roughness flow occurs when the roughness elements are so far apart that the wakes at each element are completely developed and dissipated before the next element is reached. In such flow the wall region, and accordingly the velocity profile, is deformed at each element.

In addition to the above classification, the transitional flow pattern between wake-interference flow and isolated-roughness flow can be introduced. In such flow the wall region is not uniform along the flow. For convenience sake, this transitional flow is called incomplete wake-interference flow, and the flow with uniform wall region is called complete wake-inerference flow. If the wall region is not uniform, the constant M

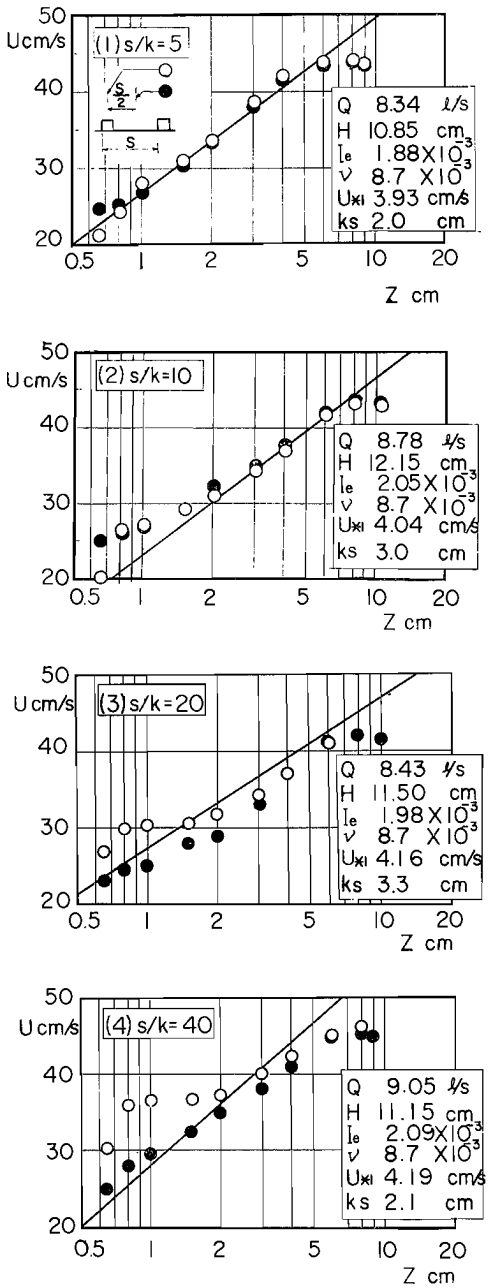

Fig. 3. Velocity profiles on the strip roughness

in eq (1) should be defined as an average over the spacing of the roughness elements. The difference in these flow patterns must be caused by various resistance characteristics

The strip roughness may produce these typically different flow patterns since the roughness elements traverse the flow with constant spacing. Fig. 3 (1)-(4) shows some results of the velocity measurements. In the figures the symbol ○ indicates that the measurement position is right on the roughness element and the symbol ● denotes that the measurment position is located at the middle point of the roughness spacing. The deformation of the velocity profile due to the roughness element is marked as increasing s/k. Because the two profiles coincide in the case of $s/k=5$, Fig. 3(1), the complete wake-interference flow occurs when s/k is less than about 10.

In addition, the real lines in Fig. 3 show the logarithmic velocity distribution by eq (1).

(3) Drag coefficient of the strip roughness element

The classiffication of the flow patterns is to be confirmed from the drag cofficient of the roughness element because it is a significant factor for characterizing the wake at the roughness element. Drag coefficient C_D is defined in the following form :

$$C_D = D \Big/ \frac{1}{2}\rho k_0 u_0^2, \tag{3}$$

in which D is drag force, k_0 is projected height of the body to the flow, u_0 is characteristic velocity of the flow, and ρ is density of the fluid.

Primarily C_D is a function of the shape of the body and Reynolds number. If the body is angular shaped and the separate point of the flow is fixed, Reynolds number becomes unimportant. Since the strip roughness elements used in the tests have a rectangular section and its crest width is small, it may be supposed that the contribution of Reynolds number to C_D is small. However, the roughness elements are placed on the flume bottom where the velocity gradient is marked. Accordingly if the average velocity U is taken as the characteristic velocity, the relative roughness height H/k should be another significant parameter for C_D. The experimental values of C_D are plotted against H/k.

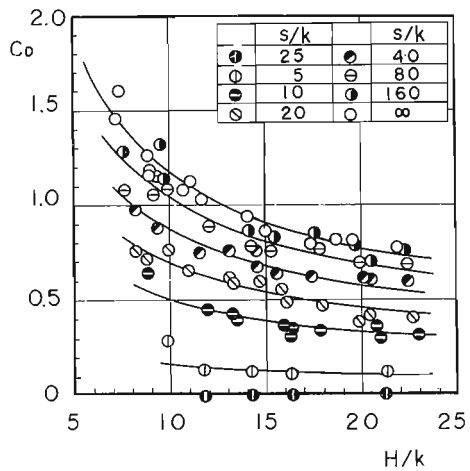

Fig. 4. Pressure drag coefficient of the strip roughness element

As was expected the correlations between C_D and H/k are good and the relative curves for each s/k may be drawn as the real lines in Fig. 4. The curve for $s/k=\infty$ indicates the isolated roughness flow because it was caused by a single roughness element. The deviations from this peculiar curve are due to the sheltering effects of the roughness elements. The experimental points of $s/k=160$ are almost all placed on the peculiar curve. Accordingly the isolated roughness flow results when s/k is larger

than 160.

(4) Datum plane of the strip roughness

The datum plane of the roughness is an important factor in the classification of the flows. In the case of the isolated roughness flow, that is, when s/k is large than 160, the datum must be set on the flume bottom because the full height of the roughness element contributes to the resistance. In such a case the strip roughness should be called the ridge roughness. On the other hand, in the case of $C_D=0$, that is, $s/k=3.5$ in this test, the datum must be set on the top of the roughness element because the height of the element no longer has any significance and the resistance depends both on the eddies caused by the gaps and the top surface of the roughness elements. In such a case the strip roughness should be called groove roughness. The position of the datum plane, therefore, must be determined according to whether the function of the roughness element is ridge or groove.

The effective drag coefficient C_D, defined from the effective flow depth, $H_e=H-c$, and the effective roughness height, $k_e=k-c$, is relative to the above C_D in the following from :

$$C_{De}=\frac{(1-c/H)^2}{1-c/k}C_D, \tag{4}$$

in which c is the sheltering height of the roughness element. Assuming that C_{De} is equal to the peculiar value of C_D for $s/k=\infty$, the values of c can be derived from eq (4). As the values of c/H are small, the ratio of C_{De} to C_D is neary equal to $1/(1-c/k)$. Then, in the diagram in which the curves in Fig. 4 are replotted into log-log scale paper, the points on the curves reach to the peculiar curve by traveling along 1 : 1 slope line with a distance $\sqrt{2}\log(c/k-1)$. Fig. 5 shows this procedure. Since replotted curved are almost parallel, the values of c/k become constant for each s/k. The results of this estimation are plotted in Fig. 6 and they indicate the function of

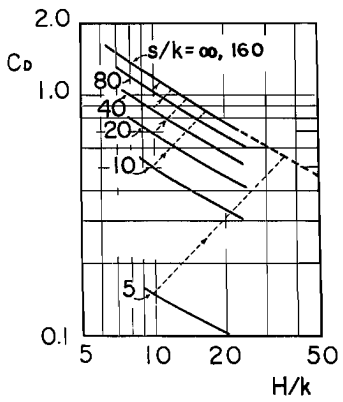

Fig. 5. Diagram for estimating the sheltering height.

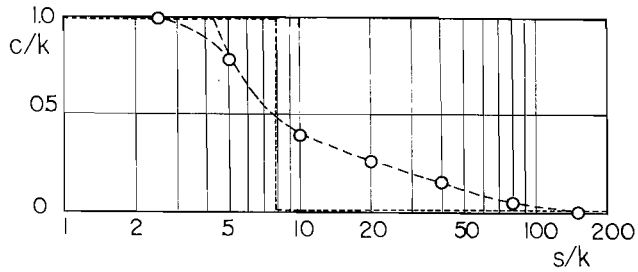

Fig. 6. Sheltering effects of the strip roughness element.

the roughness element in the transition from the groove to the ridge.

(5) Practical criterion between the ridge and the groove roughness

Although both the ridge and groove belong in the same category from the geometric view, they must be distinguished as the roughness from the position of the datum plane. As shown in Fig. 6 the roughness element possesses the nature of both the ridge and the groove when s/k is larger than 2.5 and less than 160. Accordingly, strictly speaking, the datum plane should be set on a certain middle height of the element. However, for the practical purpose, it is convenient and useful to decide the datum plane either on the bottom or the top of the roughness element. If the transition is ignored, the ridge roughness may be defined as more emphatic in nature than the nature of the groove. Similarly the groove roughness is that the nature of the groove is more emphatic than the nature of the ridge. By this definition, the practical criterion between the ridge and the groove roughness is given as $c/k=8$ for the strip roughness used in this test. The dotted line drawn in Fig. 6 shows this practical criterion. Owing to the sheltering effects, the smaller longitudinal roughness spacing causes a higher resistance for $s/k>8$ and less resistance for $s/k<8$. Therefore the above criterion corresponds to the condition which is to produce the maximum resistance. Illustrating other investigations[1),7),8)] the variations of the equivalent sand roughness with the relative longitudinal roughness spacing are shown in Fig. 7. They indicate also that the maximum resistance is produced at about $s/k=8$.

Besides, the choice of the datum plane must be consistent with the resistance character, that is, the equivalent sand roughness approaches a

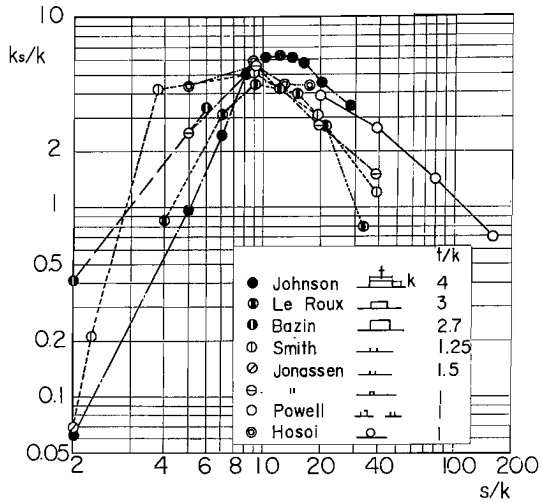

Fig. 7. Variations of the equivalent sand roughness with the relative longitudinal spacing— Bazin and Powell took the datum plane on the flume bottom, Hosoi took the datum plane on the middle height of the ridge element, and Johnson and others took the datum plane on the top of the ridge element.

constant as the flow pattern approaches the complete wake-interference flow. If the datum plane is taken on the top of ridge element instead of the ridge element instead of the flume botton, the experimental points in Fig. 2 are rewritten as shown in Fig. 8.

It may be observed that the fitness of the constant k_s curve for the experimental points in Fig. 8(1) is better than that in Fig. 2(6) for $s/k=5$. On the other hand,

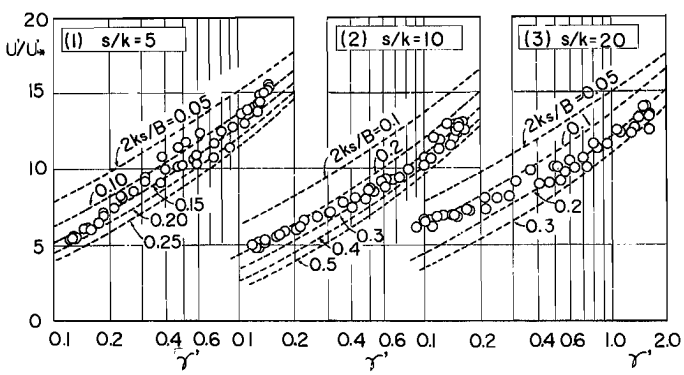

Fig. 8. Relations between U'/U_*' and γ' for various s/k

the fitness of the constant k_s curve for experimental points in Fig. 8(2), (3) is worse than that in Fig. 2 (5),(4) for $s/k=10$ and 20. Accordingly the practical criterion, $s/k=8$, is consistent with the classification of the flow patterns. It may be concluded that the ridge roughness causes the

incomplete wake-interference flow and isolated roughness flow and that the groove roughness causes the complete wake-interference flow and the skimming flow.

(2) Empirical resistance formula for the ridge roughness

As the resistance formula is derived from the velocity distribution, the problem is how to find the coefficient M in eq (1). The main factors on the behavior of the wall region may be the flow depth H, the ridge height k, the ridge spacing s, and the ridge thickness t. When the wall region has a nature somewhat similar to the laminar sublayer, Reynolds number becomes a significant factor. However, in this case it may be neglected as a result of the fact that the pressure drag coefficients were obviously not influenced by the Reynolds number. Based on the concept of dimensional analysis, the following relationship may be given :

$$Mk=\phi(H/k,\ s/k,\ t/k)$$

or using the equivalent sand roughness k_s defined by eq (2),

$$k_s/k=30/\phi(H/k,\ s/k,\ t/k).$$

In the tests t/k was held constant and H should be replaced with the hydraulic radius of the flume bottom R_1. Accordingly,

$$k_s/k=30/\phi_1(R_1/k,\ s/k). \quad (5)$$

The experimental relations corresponding to eq (5) are shown in Fig. 9.

Assuming the exponential from to the function ϕ_1 as

$$k_s/k=30/m(R_1/k)^{\theta}, \quad (6)$$

the experimental values of the coefficient m and exponent θ are obtained from Fig. 9. Fig. 10 shows the average values of m and θ at each s/k corresponding to the lines in

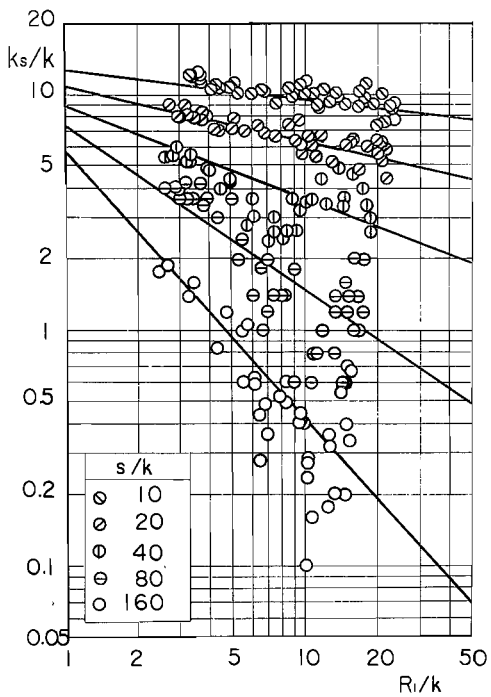

Fig. 9. Relations between k_s/k and R_1/k

Fig. 9. The empirical relationships for these are given as

$$m=0.79(s/k)^{-0.26} \text{ and } \theta=0.02(s/k)^{0.8}. \tag{7}$$

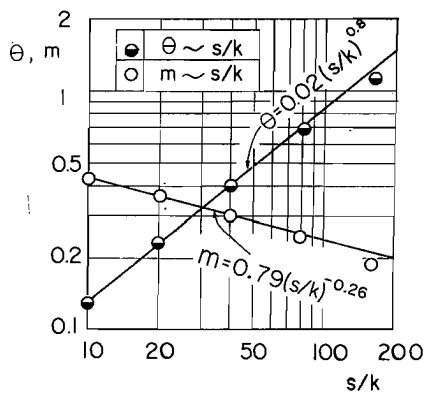

Fig. 10 Values of m and θ.

The points for $s/k=160$ in Fig. 10 are slightly apart from the lines of eq (7). This may be interpreted from the translation of the flow pattern from the incomplete wake-interference flow to the isolated roughness flow at $s/k=160$.

Substituting eq (6) and eq (7) for the logarithmic resistance law, the resistance factor from the two-dimensional flow is written in the following form :

$$U/U_*=1.5\log_{10}(s/k)-19.1+\{5.75+0.12(s/k)^{0.8}\}\log_{10}(H/k). \tag{8}$$

This is the empirical formula for the ridge roughness with the incomplete wake-interference flow, $8<s/k<160$.

(7) Fitness of the empirical formula for the ridge roughness for other investigations

R. W. Powell[5),6)] conducted investigations on the strip roughness which consisted of 1/4″ and 1/8″ square cross-sectional elements. The flows in his experiments belonged in the category of the incomplete wake-interference flow because the relative roughness spacing s/k ranged from 20 to 160. He proposed the other empirical formula using a new parameter of the roughness instead of the equivalent sand roughness. Rewritting his formula in the dimensionless expression,

$$U/U_*=7.41\log_{10}(R/\epsilon). \tag{9}$$

The appearance of the incomplete wake-interference flow would be a reason why the new parameter ϵ was needed.

Referring to his original date for the mild slope flume, although his investigation extended to supercritical flow region, the relations between U/U_* and R/k for each s/k are plotted in Fig. 11. The curves in Fig. 11 show the relationships of these based on the author's empirical formula. Strictly speaking, the agreement between the points and the

curves is not complete. A cause of the disagreements may be the fact that the disturbances due to the roughness on the botton and the side walls interfere with each other extremely because the flume is relatively small. However, the disagreements are not so excessive as to deny completely the fitness of the author's curves. For the practical accuracy, such a degree of disagreement may be allowable enough.

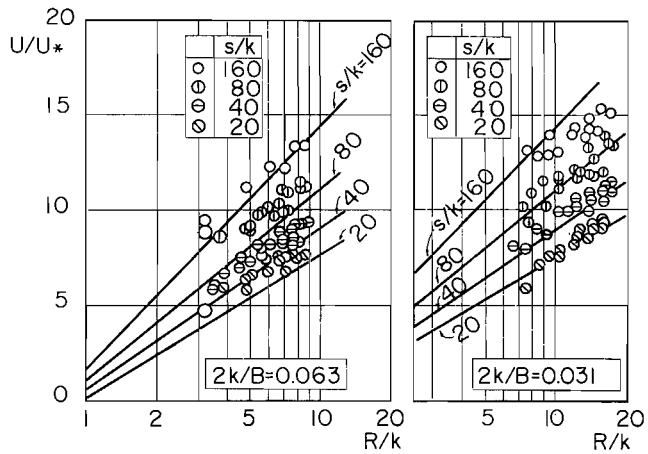

Fig. 11. Relations between U/U_* and R/k after R. W. Powell

As the second example, the experimental data on the triangular sectional ridge roughness obtained in the investigation of W. E. S.[9], are plotted in Fig. 12 after the same fashion. The curves based on the author's empirical formula, agree with these experimental points, regardless of the difference of the shape of the roughness elements and the material of the

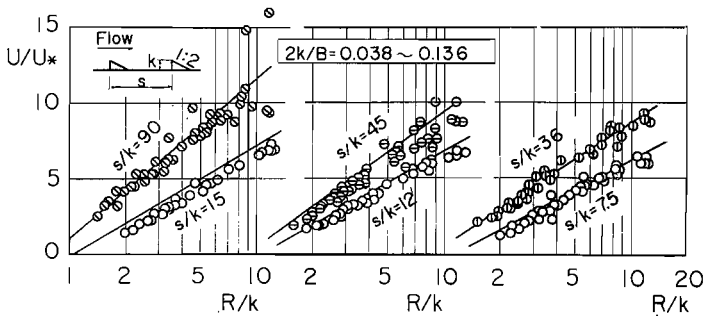

Fig. 12. Relations between U/U_* R/k after W. E. S.

flumes.

From the above two examples it may be conclued that the author's empirical formula for the ridge roughness with the incomplete wake-interference flow is validated.

(8) **The resistance character of the groove roughness**

The roughness effects observed in the second tests, in which the strip elements were set on the bottom close together and the relative groove roughness s/b ranged from 2 to 16, are shown in Fig. 13(2)—(4) after

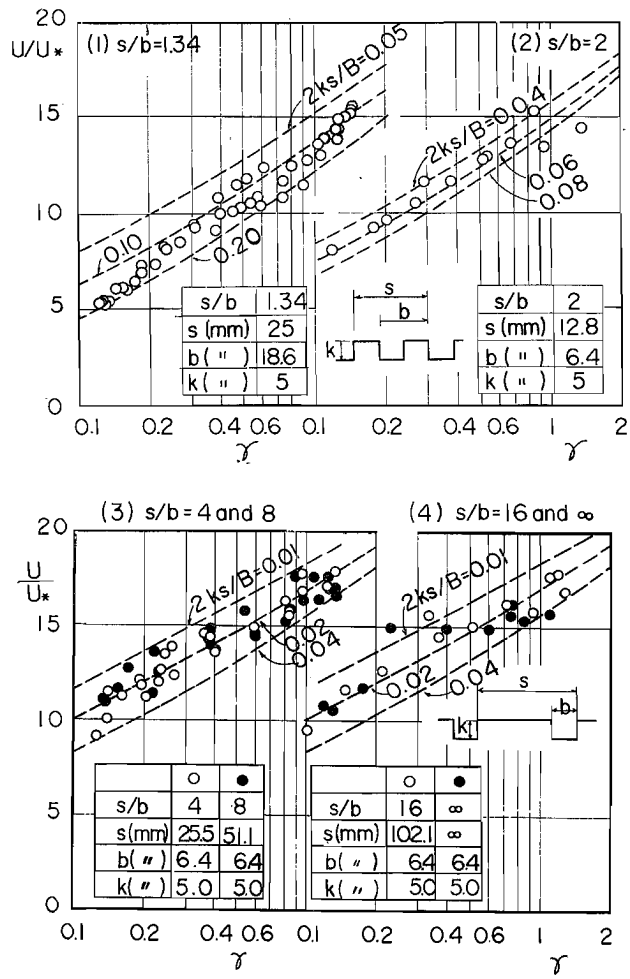

Fig. 13. Relations between U/U_* and γ for various s/b

the same fashion as those in Fig. 2. Fig. 13(1) shows that of the groove roughness in the first tests, Fig. 8(1). It is apparent that the resistance characters of the groove roughness are similar to those of the sand grain roughness. From these results the relations between the equivalent sand roughness and the hydraulic radius of the flume bottom are obtained as shown in Fig. 14. The data of J. W. Johnson's experiment[7] in which rectangular cross sectional elements were used are added as a complement. Although the points are scattered, especially for $s/b>4$, the equivalent sand roughness may be given as a constant for each s/b as shown by the broken lines.

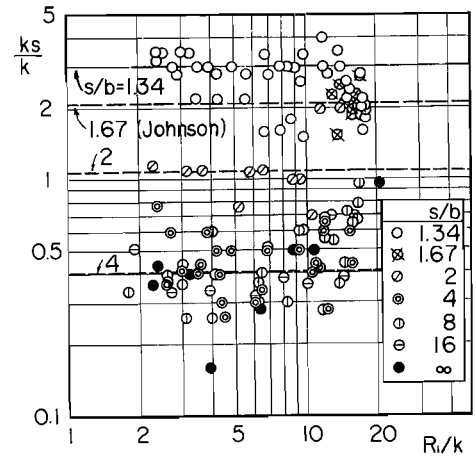

Fig. 14. Relations between K_s/K and R_1/K

The skimming flow, by Morris classification, will result when the dead water or the stable vortex is caused in the groove. However, if the longitudinal width of the top surface is small in comparison with the groove width, it is doubuful that the dead water or the stable vortex is caused in the groove. In such a case the complete wake-interference flow will result rather than the skimming flow.

The author expected in the begining that the skimming flow would occur for large s/b. However, it was apparent that the experimental values of k_s were independent of the flow depth. Even for $s/b=\infty$, in which the grooves were filled up entirely, the smooth surface flow was not observed as shown in Fig. 14. This absurdity may be caused by the irregularities of the top surface of the wooden bars which fill up the grooves. According to Morris, the increment of the resistance coefficient due to the groove element is given as

$$f-f_s=0.05(p_r/p_o)(b/s), \tag{10}$$

in which f is total resistance coefficient $[=8/(U/U_*)^2]$, f_s is resistance cofficient of the top surface, p_o is the wetted perimeter, and p_r is the roughened perimeter. Based on eq (10), the increment of the resisance

coefficient due to the groove element in the author's tests would be about $5\times10^{-2}\sim10^{-2}$ for $s/b=4$ and it would become small in inverse proportion to the increase of s/b. On the other hand, the corresponding total resistance coefficient in the tests ranged from about 2.5×10^{-2} to 8×10^{-2}. Consequently the contribution of the groove element to the resistance may be neglected practically for $s/b>4$ in this test.

(9) Empirical formula for the groove roughness

The essential difference between the groove roughness and the ridge roughness is that the wakes at the ridge elements are restricted by the grooves. Accordingly the groove width b may be an important factor. Fig. 15 shows the relations between k_s/k and s/b, with other added experimental data shown in Fig. 7. Assuming a straight line for representing these experimental points in Fig. 15, the empirical formula for k_s is given in the following exponential form.

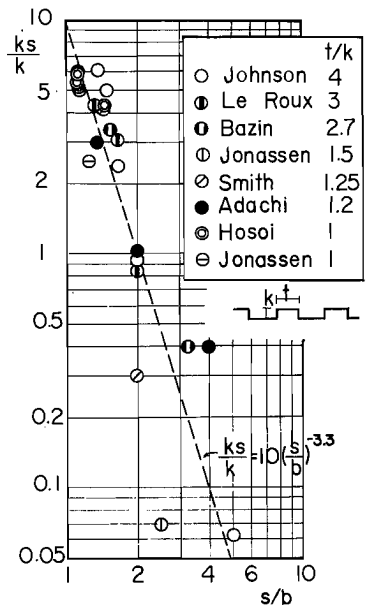

Fig. 15. Relationship between k_s/k and s/b

$$k_s/k=10(s/b)^{-3.3}. \tag{11}$$

Inserting the above relationship into the logarithmic resistance law, the resistance factor for the two-dimensional flow is written as :

$$U/U_*=0.25+19.0\log_{10}(s/b)+5.75\log_{10}(H/k). \tag{12}$$

This is the empirical roughness formula for the groove roughness with complete wake-interference flow.

If s/b approaches 1, the strip roughness will be the the ridge roughness. According to the previous practical criterion between the ridge and the groove roughess, the lower limit of the value of s/b for the groove roughness in the tests may be

$$\frac{s}{b}=\frac{s/k-t/k}{s/k}=\frac{8-6.4/5.0}{8}=1.2$$

Besides, if s/b approaches infinity, the value of U/U_* evaluted by

eq(12) also become infinity. However, there must be an upper limit for U/U_* because the total resistance is never less than the friction resistance of the top surface. Since the contribution of the groove element to the resistance becomes negligible as increasing s/b, the friction resistance of the top surface can be considered as the upper limit for U/U_*. In this test, $k_s/k \geq 0.4$, accordingly $s/b \leq 2.6$, may be the upper limit.

Conclusions

This experimental study may be summarized as follows ;

(1) The equivalent sand roughness does not always correspond to the roughness pattern and varies with the flow depth. It may be considered as a measure for the wall region consisting of the intense vorticities caused by the rougbness elements.

(2) It may be needed for representing the roughness effect of the strip elements with the relative spacing s/k ranged from 8 to 160, to introduce the transitional flow pattern between the wake-interference flow and the isolated roughness flow, namely incomplete wake-interference flow, in which the wall region is not uniform along the flow.

(4) The condition of $s/k=8$ in the strip roughness may be a practical criterion for distinguishing the ridge and the groove roughness. In the case of the ridge roughness the datum plane is set on the bottom of the flume and in the case of the groove roughness the datum plane is set on the top of the ridge element. This criterion corresponds also to the condition which is to produce the maximum resistance with the strip elements

(4) The empirical logarithmic roughness formula for the ridge rough ness with the incomplete wake-interference flow was developed in terms of the relative roughness heigh H/k and the relative ridge spacing s/k, as eq(8). The similar empirical formula for the groove roughness with the complete wake-interference flow was derived as eq (12) in terms of the relative roughness height H/k and the relative groove spacing s/b.

Acknowledgements

The author wishes to express his deep thanks to Prof. Katsumasa Yano, Prof. Tojiro Ishihara, and Prof. Yuichi Iwagaki for their kind guidance

and invaluable help throughout the course of the present study.

References

1) Powell, R. W. Flow in a channel of definite roughness, Trans. A. S. C. E., Vol. 111, 1964, pp. 531—566.
2) Powell, R. W. Resistance to flow in rough channels, Trans. A. G. U., Vol, 31. No. 4, Aug. 1950, pp. 575—582.
3) Robinson, A. R. and Albertson, M. L. . Artificial roughness standard for open channels, Trans. A. G. U., Vol. 33, No. 6, Dec. 1952. pp. 881—888.
4) Morris, H. M. Flow in rough conduits, Trans. A. S. C. E., 1955, pp. 373—410.
5) Morris, H. M, Design methods for flow in rough conduits, Proc. A. S. C. E., Vol. 85, July 1959, pp. 43—62.
6) Adachi, S. The effects of side walls in restangular croos sectional channel, Trans. of J. S. C. E., No. 81 May 1962, pp. 17—26.
7) Johnson, J. W. : Rectangular artificial roughness in open channels, Trans. A. G. U., 1944, pp. 906—914.
8) Hosoi, M. : On the velocity distribution and the frictional resistance of turbulent flow in open channels, Dobokukenkyu, Vol. 1, 1951, pp. 79—132.
9) Waterways Experiment Station : Roughness standards for hydraulic models —Report No. 1, Study of finite boundary roughness in rectangular flumes, Corps of U. S. Army, Tech. Memo., No. 2—364. June 1953.

Publications of the Disaster Prevention Research Institute

The Disaster Prevention Research Institute publishes reports of the research results in the form of bulletins. Publications not out of print may be obtained free of charge upon request to the Director, Disaster Prevention Research Institute, Kyoto University, Kyoto, Japan.

Bulletins :

No. 1 On the Propagation of Flood Waves by Shoitiro Hayami, 1951.

No. 2 On the Effect of Sand Storm in Controlling the Mouth of the Kiku River by Tojiro Ishihara and Yuichi Iwagaki, 1952.

No. 3 Observation of Tidal Strain of the Earth (Part I) by Kenzo Sassa, Izuo Ozawa and Soji Yoshikawa. And Observation of Tidal Strain of the Earth by the Extensometer (Part II) by Izuo Ozawa, 1952.

No. 4 Earthquake Damages and Elastic Properties of the Ground by Ryo Tanabashi and Hatsuo Ishizaki, 1953.

No. 5 Some Studies on Beach Erosions by Shoitiro Hayami, Tojiro Ishihara and Yuichi Iwagaki, 1953.

No. 6 Study on Some Phenomena Foretelling the Occurrence of Destructive Earthquakes by Eiichi Nishimura, 1953.

No. 7 Vibration Problems of Skyscraper. Destructive Element of Seismic Waves for Structures by Ryo Tanabashi, Takuzi Kobori and Kiyoshi Kaneta, 1954.

No. 8 Studies on the Failure and the Settlement of Foundations by Sakurō Murayama, 1954.

No. 9 Experimental Studies on Meteorological Tsunamis Traveling up the Rivers and Canals in Osaka City by Shoitiro Hayami, Katsumasa Yano, Shohei Adachi and Hideaki Kunishi, 1955.

No.10 Fundamental Studies on the Runoff Analysis by Characteristics by Yuichi Iwagaki, 1955.

No.11 Fundamental Considerations on the Earthquake Resistant Properties of the Earth Dam by Motohiro Hatanaka, 1955.

No.12 The Effect of the Moisture Content on the Strength of an Alluvial Clay by Sakurō Murayama, Kōichi Akai and Tōru Shibata, 1955.

No.13 On Phenomena Forerunning Earthquakes by Kenzo Sassa and Eiichi Nishimura, 1956.

No.14 A Theoretical Study on Differential Settlements of Structures by Yoshitsura Yokoo and Kunio Yamagata, 1956.

No.15 Study on Elastic Strain of the Ground in Earth Tides by Izuo Ozawa, 1957.

No.16 Consideration on the Mechanism of Structural Cracking of Reinforced Concrete Buildings Due to Concrete Shrinkage by Yoshitsura Yokoo and S. Tsunoda. 1957.

No.17 On the Stress Analysis and the Stability Computation of Earth Embankments by Kōichi Akai, 1957.

No.18 On the Numerical Solutions of Harmonic, Biharmonic and Similar Equations by the Difference Method Not through Successive Approximations by Hatsuo Ishizaki, 1957.

No.19 On the Application of the Unit Hydrograph Method to Runoff Analysis for Rivers in Japan by Tojiro Ishihara and Akiharu Kanamaru, 1958.

No.20 Analysis of Statically Indeterminate Structures in the Ultimate State by Ryo Tanabashi, 1958.

No.21 The Propagation of Waves near Explosion and Fracture of Rock (I) by Soji Yoshikawa, 1958.

No.22 On the Second Volcanic Micro-Tremor at the Volcano Aso by Michiyasu Shima, 1958.

No.23 On the Observation of the Crustal Deformation and Meteorological Effect on It at Ide Observatory and On the Crustal Deformation Due to Full Water and Accumulating Sand in the Sabo-Dam by Michio Takada, 1958.

No.24 On the Character of Seepage Water and Their Effect on the Stability of Earth Embankments by Kōichi Akai, 1958.

No.25 On the Thermoelasticity in the Semi-infinite Elastic Soid by Michiyasu Shima, 1958.

No 26 On the Rheological Characters of Clay (Part 1) by Sakurō Murayama and Tōru Shibata, 1958.

No.27 On the Observing Instruments and Tele-metrical Devices of Extensometers and Tiltmeters at Ide Observatory and On the Crustal Strain Accompanied by a Great Earthquake by Michio Takada, 1959.

No.28 On the Sensitivity of Clay by Shinichi Yamaguchi, 1959.

No.29 An Analysis of the Stable Cross Section of a Stream Channel by Yuichi Iwagaki and Yoshito Tsuchiya, 1959.

No.30 Variations of Wind Pressure against Structures in the Event of Typhoons by Hatsuo Ishizaki, 1959.

No.31 On the Possibility of the Metallic Transition of MgO Crystal at the Boundary of the Earth's Core by Tatsuhiko Wada, 1960.

No.32 Variation of the Elastic Wave Velocities of Rocks in the Process of Deformation and Fracture under High Pressure by Shogo Matsushima, 1960.

No.33 Basic Studies on Hydraulic Performances of Overflow Spillways and Diversion Weirs by Tojiro Ishihara, Yoshiaki Iwasa and Kazune Ihda, 1960.

No.34 Volcanic Micro-tremors at the Volcano Aso by Michiyasu Shima, 1960.

No.35 On the Safety of Structures Against Earthquakes by Ryo Tanabashi, 1960.

No.36 On the Flow and Fracture of Igneous Rocks and On the Deformation and Fracture of Granite under High Confining Pressure by Shogo Matsushima, 1960.

No.37 On the physical properties within the B-layer deduced from olivine-model and on the possibility of polymorphic transition from olivine to spinel at the 20° Discontinuity by Tatsuhiko Wada, 1960.

No.38 On Origins of the Region C and the Core of the Earth ——Ionic-Intermetallic-Metallic Transition Hypothesis—— by Tatsuhiko Wada, 1960.

No.39 Crustal Stucture in Wakayama District as Deduced from Local and Near Earthquake Observations by Takeshi Mikumo, 1960.

No.40 Earthquake Resistance of Traditional Japanese Wooden Structures by Ryo Tanabashi, 1960.

No.41 Analysis With an Application to Aseismic Design of Bridge Piers by Hisao Goto and Kiyoshi Kaneta, 1960.

No.42 Tilting Motion of the Ground as Related to the Volcanic Activity of Mt. Aso and Micro-Process of the Tilting Motion of Ground and Structure by Yoshiro Itō 1961.

No.43 On the Strength Distribution of the Earth's Crust and the Upper Mantle, and

the Distribution of the Great Earthquakes with Depth by Shogo Matsushima, 1961

No.44 Observational Study on Microseisms (Part 1) by Kennosuke Okano, 1961.

No.45 On the Diffraction of Elastic Plane Pulses by the Crack of a Half Plane by Michiyasu Shima, 1961.

No.46 On the Observations of the Earth Tide by Means of Extensometers in Horizontal Components by Izuo Ozawa, 1961.

No.47 Observational Study on Microseisms (Part 2) by Kennosuke Okano, 1961.

No.48 On the Crustal Movement Accompanying with the Recent Activity on the Volcano Sakurajima (Part 1) by Keizo Yoshikawa, 1961.

No.49 The Ground Motion Near Explosion by Soji Yoshikawa, 1961.

No.50 On the Crustal Movement Accompanying with the Recent Activity of the Volcano Sakurajima (Part 2) by Keizo Yoshikawa, 1961.

No.51 Study on Geomagnetic Variation of Telluric Origin Part 1 by Junichiro Miyakoshi, 1962.

No.52 Considerations on the Vibrational Behaviors of Earth Dams by Hatsuo Ishizaki and Naotaka Hatakeyama, 1962.

No.53 Some Problems on Time Change of Gravity (Parts 1 and 2) by Ichiro Nakagawa, 1962.

No.54 Nature of the Volcanic Micro-Tremors at the Volcano Aso, Part 1. Observation of a New Type of Long-Period Micro-Tremors by Long-Period Seismograph by Kosuke Kamo, 1962.

No.55 Nature of the Volcanic Micro-Tremors at the Volcano Aso, Part 2. Some Natures of the Volcanic Micro-Tremors of the 1st kind at the Volcano Aso by Kosuke Kamo, 1962.

No.56 Nonlinear Torsional Vibration of Structures due to an Earthquake by Ryo Tanabashi, Takuji Kobori and Kiyoshi Kaneta, 1962.

No.57 Some Problems on Time Change of Gravity (Parts 3, 4 and 5) by Ichiro Nakagawa, 1962.

No.58 A Rotational Strain Seismometer by Hikaru Watanabe, 1962.

No.59 Hydraulic Model Experiment Involving Tidal Motion (Parts 1, 2, 3 and 4) by Haruo Higuchi, 1963.

No.60 The Effect of Surface Temperature on the Crustal Deformations by Shokichi Nakano, 1963.

No.61 An Experimental Study on the Generation and Growth of Wind Waves by Hideaki Kunishi, 1963.

No.62 The Crustal Deformations due to the Source of Crack Type (1) by Shokichi Nakano, 1963.

No.63 Basic Studies on the Criterion for Scour Resulting from Flows Downstream of an Outlet by Yoshito Tsuchiya, 1963.

No.64 On the Diffraction of Elastic Plane Pulses by a Crack of a Half Plane (Three Dimensional Problem) by Michiyasu Shima, 1963.

No.65 A Study on Runoff Pattern and its Characteristics by Tōjiro Ishihara and Takuma Takasao, 1963.

No.66 Application of Extreme Value Distribution in Hydrologic Frequency Analysis by Mutsumi Kadoya, 1964.

No.67 Investigation on the Origin Mechanism of Earthquakes by the Fourier Analysis of Seismic Body Waves (1) by Yoshimichi Kishimoto, 1964.

No.68 Aseismic Design Method of Elasto-Plastic Building Structures by Takuji

Kobori and Ryoichiro Minai, 1964.

No.69 On the Artificial Strip Roughness by Shōhei Adachi, 1964.

Bulletin No. 69 Published March, 1964

昭和 39 年 3 月 20 日 印 刷
昭和 39 年 3 月 25 日 発 行

編輯兼
発行者 京都大学防災研究所

印刷者 山 代 多 三 郎
京都市上京区寺之内通小川西入

印刷所 山代印刷株式会社